Ab Initio Study of Trimethyl Phosphate: Conformational Analysis, Dipole Moments, Vibrational Frequencies, and Barriers for Conformer Interconversion

Lisa George,[†] K. S. Viswanathan,*[,‡] and Surjit Singh[†]

Regional Sophisticated Instrumentation Center, Indian Institute of Technology, Madras 600 036, India, and Materials Chemistry Division, Indira Gandhi Center for Atomic Research, Kalpakkam 603 102, India

Received: August 20, 1996; In Final Form: December 30, 1996[⊗]

Ab initio molecular orbital calculations on trimethyl phosphate (TMP) were done using 6-31G* and 6-31G** basis sets, both at RHF and MP2 levels of theory. We located three minima corresponding to C_3, C_1, and C_s symmetries, given in order of increasing energies. At the MP2/6-31G** level, the energy difference between the C_3 and C_1 conformers was 0.56 kcal/mol, while that between the C_3 and C_s was 1.43 kcal/mol. Our observations are at variance with an earlier ab initio calculation, employing smaller basis sets, STO-3G* and 4-31G*, which had reported that the C_1 conformer was the lowest in energy. Furthermore, the earlier calculation did not report the occurrence of a minimum corresponding to the C_s symmetry. Vibrational frequency calculations were done at the HF and MP2 levels. The computed frequencies were found to compare well with experimental vapor phase and matrix isolation data reported earlier, leading to a definitive assignment of the infrared features of TMP. The barrier for conformer interconversion, $C_1 \leftrightarrow C_3$, was also computed at the HF/6-31G** and MP2/6-31G** levels. At the MP2/6-31G** level the $C_1 \rightarrow C_3$ barrier was found to be 2.20 kcal/mol, while that for $C_3 \rightarrow C_1$ was 2.76 kcal/mol.

Introduction

Organic phosphates play an important role in a variety of chemical processes, such as in biological chemistry, solvent extraction processes, and insecticides in agriculture applications, to name just a few. The spectroscopy of organic phosphates has proved to be intriguing, and even a simple phosphate such as trimethyl phosphate (TMP) has eluded a detailed and unambiguous assignment to date. A controversial aspect in any discussion concerning the phosphates has been their molecular structure. Conformers with different structures have been proposed for TMP on the basis of experimental and computational exercises.

One of the earliest works on the spectroscopy of TMP is that of Mortimer.[1] Mortimer concluded in that study that TMP exists in at least two different conformations, of which the conformer with the higher P═O stretching frequency was the lower in energy, with probably a C_3 symmetry. He did not specifically discuss the structure of the higher energy conformer. Then followed the work of Maiants et al.[2] and Popov et al.,[3] who generally agreed with the findings of Mortimer and added that the higher energy conformer had a C_{3v} symmetry. While these studies mainly dealt with TMP in the liquid and solid state, Herail,[4] using gas phase IR data on TMP, also concluded that the two conformers have C_{3v} and C_3 symmetries. Using NMR and classical potential function calculations, Khetrapal et al.[5] arrived at two possible conformations for TMP that both had C_3 geometries but with different O═P−O−C torsional angles.

For the first time, Van Wazer and Ewig[6] applied ab initio molecular orbital computations to the TMP problem. They concluded that most of the geometries arrived at in earlier works had unduly high symmetry. Their calculations at the HF/STO-3G* and HF/4-31G* level yielded geometries that had C_1 and C_3 symmetries. They computed an energy difference of 1 kcal/mol between the two conformations (at the HF/4-31G* level), with the C_1 being lower in energy than C_3. Later, Taga et al.[7] concluded that TMP coexisted in three different conformations, with C_3, C_1, and C_s symmetries.

For the first time, Lisa et al.[8] published matrix isolation IR spectra of TMP trapped in nitrogen and argon matrices. Peaks due to the different conformers were clearly discerned in these spectra, which were assigned on the basis of the conclusions of Herail. In a recent work, Sablinskas et al.[9] have performed ab initio calculations on TMP at the HF/6-31G* level. Their conclusions were identical with those of Van Wazer and Ewig, namely that the C_1 conformer of TMP was more stable than the C_3. Recently, Vidya et al.,[10] using supersonic beam−matrix isolation spectroscopy, assigned vibrational features corresponding to the different conformers of TMP, in the region of the P═O and P−O−C vibrations.

In spite of the large amount of literature on TMP, the structures of the conformers are not clearly understood. Hence we decided to perform ab initio computations on TMP using the 6-31G* and 6-31G** basis sets, both at the HF level and by employing the Moller−Plesset perturbation correction to second order (MP2), to estimate the effect of electron correlation.

We have also performed vibrational frequency calculations to corroborate the assignments of Vidya et al.[10] Vibrational frequencies for all three conformers were calculated at the HF/6-31G* and HF/6-31G** levels. For the C_3 and C_1 conformers, vibrational frequencies were also computed at the MP2/6-31G* level.

Except for gross estimates based on matrix isolation work,[9] there is no experimental or computed value for the barrier for conformer interconversion in TMP. We have therefore computed the energy barrier for the conversion between the two major conformers, C_1 and C_3.

Computational Methods

Ab initio molecular orbital calculations were performed using the Gaussian 92 program[11] on a Hewlett-Packard Workstation (model 715/64). Geometry optimizations were done both at

* Author to whom correspondence should be addressed.
[†] Indian Institute of Technology.
[‡] Indira Gandhi Center for Atomic Research.
[⊗] Abstract published in *Advance ACS Abstracts,* February 15, 1997.

S1089-5639(96)02557-1 CCC: $14.00

the HF and MP2 level with analytical gradients, using 6-31G* and 6-31G** basis sets. All geometrical parameters were allowed to be optimized, and no structural constraints were imposed during the optimization process. Vibrational frequencies were calculated at the HF level, for all the geometries, using analytical derivatives, with the 6-31G* and 6-31G** basis sets. Frequency calculations at the MP2 level were done only with the 6-31G* basis set, using numerical derivatives to circumvent disk storage constraints.

Results and Discussion

Molecular Geometry. We performed all geometry optimizations independently in both the basis sets mentioned above, using the full optimization option, both at the HF and MP2 levels. In each case, we obtained three minima corresponding to conformations that differed mainly in the dihedral angle between the O═P−O and P−O−C planes. The geometries correspond to C_3, C_1, and C_s symmetries. That these geometries correspond to energy minima was confirmed by a vibrational analysis, which yielded all positive frequencies for these structures. The molecular parameters obtained at the MP2/6-31G** level, defining the three geometries, are given in Table 1. The corresponding structures are shown in Figure 1.

The relative energies of the conformers, at the HF and MP2 levels, obtained using both basis sets (6-31G* and 6-31G**) are shown in Table 2. The relative energies shown in the table were corrected for zero-point energies. The zero-point energy of each conformer for a given basis set was computed using the frequencies obtained at the HF level. The value thus obtained was scaled by 0.92, a factor that brings the computed HF frequencies in agreement with vapor phase values.

The C_3 conformer, with O═P−O−C torsional angles of 45°, was the most stable. The next higher energy conformer corresponded to a C_1 symmetry, followed by the C_s geometry. The energy differences between the different conformers varied, and not surprisingly, with the basis sets and the level of theory employed. At the highest level of theory that we used, namely MP2/6-31G**, the energy difference between the C_3 and C_1 was 0.56 kcal/mol, while that between C_3 and C_s was 1.43 kcal/mol. However, the structure of the conformers did not vary significantly when different basis sets were used.

Our finding that the C_3 conformer is the lowest in energy is at variance with the observations of Van Wazer and Ewig, who, using smaller basis sets, found the C_1 conformer to be the most stable. Such reversal in energy ordering of the conformers, on expanding to a larger basis set, has often been observed.[6] The optimized structures that we obtained for the C_3 and C_1 conformers were not significantly different from those obtained in the earlier study.

It must also be noted that Van Wazer and Ewig did not report the occurrence of a minimum corresponding to the C_s conformer.

The energy ordering that we obtained for the conformers of TMP is also at variance with the findings of Sablinskas et al., who reported the C_1 geometry to be more stable than the C_3 by ~1 kcal/mol at the HF/6-31G* level. As can be seen from Table 2, at this level of theory the C_3 conformer is the lowest energy form. However, the *energy difference* between the two conformers that we obtained agreed with that reported by Sablinskas et al.

We also searched the potential surface, at the MP2/STO-3G* level, for a minimum corresponding to a C_{3v} symmetry, with the O═P−O−C torsional angle of 0°, since this was one of the geometries predicted by Herail. However, while this C_{3v} geometry did correspond to a stationary point, it turned out to be saddle point structure, as revealed by a vibrational analysis.

TABLE 1: Structural Parameters[a] of the Three Conformers and the Transition State (TS) of TMP Computed at the MP2/6-31G Level**

parameter	C_3	TS	C_1	C_s
$P{=}O^0$	1.4852	1.4827	1.4789	1.4789
$P{-}O^1$	1.6078	1.6099	1.6092	1.6111
$P{-}O^2$	1.6077	1.6179	1.6238	1.6112
$P{-}O^3$	1.6077	1.6055	1.6038	1.6183
$O^1{-}C_1$	1.4442	1.4443	1.4435	1.4459
$O^2{-}C^2$	1.4445	1.4433	1.4444	1.4459
$O^3{-}C_3$	1.4445	1.4399	1.4425	1.4416
$C_1{-}H^1$	1.0880	1.0879	1.0879	1.0889
$C_1{-}H^2$	1.0843	1.0845	1.0845	1.0864
$C_1{-}H^3$	1.0871	1.0874	1.0877	1.0841
$C^2{-}H^4$	1.0880	1.0887	1.0890	1.0889
$C^2{-}H^5$	1.0842	1.0849	1.0849	1.0840
$C^2{-}H^6$	1.0870	1.0870	1.0868	1.0864
$C_3{-}H^7$	1.0880	1.0866	1.0881	1.0877
$C_3{-}H^8$	1.0842	1.0848	1.0847	1.0845
$C_3{-}H^9$	1.0870	1.0870	1.0867	1.0877
$O{=}P{-}O^1$	116.36	117.65	118.82	117.73
$O{=}P{-}O^2$	116.37	114.08	114.85	117.75
$O{=}P{-}O^3$	116.37	115.72	113.86	111.61
tor$O^2PO^0O^1$ [b]	119.98	118.10	118.39	116.05
tor$O^3PO^0O^1$	−120.00	−120.09	−119.01	−121.99
PO^1C_1	116.60	116.36	116.82	115.63
PO^2C^2	116.55	117.09	116.23	115.61
PO^3C_3	116.55	122.39	119.12	118.34
tor$O^0PO^1C_1$	45.21	49.44	55.17	−39.50
tor$O^0PO^2C^2$	45.17	38.38	37.22	40.02
tor$O^0PO^3C_3$	45.15	119.53	177.90	179.91
$O^1C_1H^1$	109.92	109.76	109.92	110.47
$O^1C_1H^2$	106.01	106.05	106.05	110.21
$O^1C_1H^3$	110.37	110.18	110.17	105.75
$O^2C^2H^4$	109.88	110.10	110.33	110.47
$O^2C^2H^5$	105.96	105.98	105.98	105.75
$O^2C^2H^6$	110.32	110.42	110.34	110.21
$O^3C_3H^7$	109.88	110.63	110.45	110.43
$O^3C_3H^8$	105.96	105.50	105.82	105.97
$O^3C_3H^9$	110.32	110.69	109.97	110.44
tor$PO^1C_1H^1$	68.28	67.57	67.27	−64.13
tor$H^1C_1O^1H^2$	118.73	118.97	119.15	121.49
tor$H^1C_1O^1H^3$	−121.63	−121.54	−121.67	−118.91
tor$PO^2C^2H^4$	68.29	71.08	66.49	64.01
tor$H^4C^2O^2H^5$	118.74	118.64	118.81	118.92
tor$H^4C^2O^2H^6$	−121.62	−121.56	−121.36	−121.46
tor$PO^3C_3H^7$	68.30	61.95	53.00	60.89
tor$H^7C_3O^3H^8$	118.74	119.25	119.19	119.36
tor$H^7C_3O^3H^9$	−121.62	−121.82	−121.59	−121.26

[a] Bond lengths are in angstroms, and bond angles are in degrees. [b] Torsional angle ABCD is defined at the angle between the planes ABC and BCD.

Dipole Moments. The dipole moments for the three conformers computed at the different levels of theory employed in this work are shown in Table 2. The lowest energy conformer has the lowest dipole moment, in keeping with a number of previous observations[6,12,13] that the less polar form always prevails. This observation has generally been explained on the basis that dipole−dipole forces align the local dipole moments in various parts of the molecule antiparallel to each other, resulting in a small molecular dipole moment.[6] However, in the calculations of Van Wazer and Ewig using smaller basis sets, the lower energy conformer had a larger dipole moment. They argued that steric interactions among the three methyl groups in the C_3 conformer caused this lower dipole moment structure to be higher in energy. Following the reversal in energy ordering of the conformers when larger basis sets, 6-31G* and 6-31G**, are used, the lower energy conformer now has the smaller dipole moment.

Using the energy differences between the conformers and the computed dipole moments, we have calculated the total dipole moment of TMP averaged over the three forms and obtained a

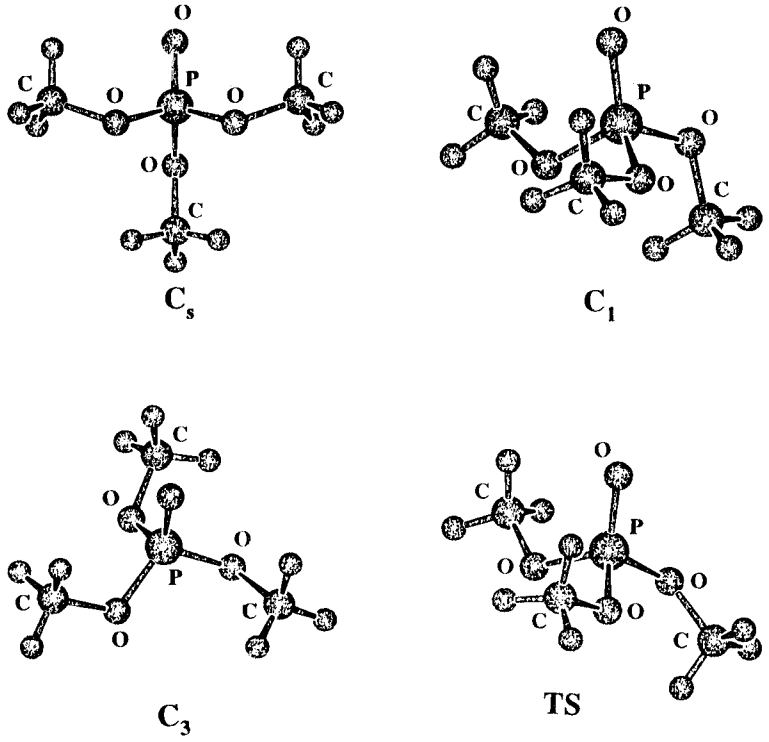

Figure 1. Structures of TMP corresponding to the three minima with C_3, C_1, and C_s symmetries and the transition state connecting the C_3 and C_1 minima, calculated at the MP2/6-31G** level.

TABLE 2: Relative Energies of the Three Conformers and Their Dipole Moments Calculated at Various Levels of Theory

		relative energy[a]		μ[b]	
basis sets	conf symmetry	HF	MP2	HF	MP2
6-31G*	C_3	0.00	0.00	1.03	0.65
	C_1	1.02	0.63	4.01	4.14
	C_s	1.95	1.50	3.24	3.30
6-31G**	C_3	0.00	0.00	1.01	0.64
	C_1	1.02	0.56	4.01	4.15
	C_s	1.95	1.43	3.22	3.28

[a] Energy relative to the C_3 conformer in kcal/mol. [b] Dipole moment in debye.

value of 3.5 D, a value that compares well with the experimental value of ~3 D obtained at room temperature in CCl_4.[12]

Vibrational Assignments. The vibrational frequencies were calculated at the HF/6-31G* and HF/6-31G** level for all three conformers, using analytical gradients. Since the two basis sets yielded frequencies that were almost identical, we will discuss the frequencies that we obtained using the 6-31G** basis only. The computed frequencies are listed in Table 3, together with the experimental values obtained using vapor phase and matrix isolation experiments from refs 8 and 10. Alongside the computed HF/6-31G** frequencies, we have given the scaled frequencies (as discussed below), to bring the computed frequencies in agreement with the matrix isolation data.

For the C_3 and C_1 conformers, we also performed frequency calculations at the MP2/6-31G* level to study the effect of electron correlation on the vibrational frequencies in TMP. Since the MP2 level frequency calculations were extremely time consuming, we did not perform these calculations for the minor conformer with C_s symmetry, nor did we perform the frequency calculation at the MP2/6-31G** level. The computed MP2/6-31G* frequencies are also shown in Table 3.

We have restricted our discussion to the modes involving the P═O and P−O−C vibrations, since these are the modes that have the largest infrared intensities in the TMP spectra. Of these, the P═O stretch is particularly important, since it is the vibration that is probed when studying TMP adducts in matrix isolation experiments.[14−16] We shall first compare the computed vibrational frequencies with vapor phase data of ref 8 and then discuss the matrix isolation data reported in refs 8 and 10.

Comparison of Vapor Phase Data with Computed Frequencies. Our frequency calculations clearly indicate that the lower energy C_3 conformer has the lower vibrational frequency for the P═O stretch. Consequently, the lower frequency infrared feature at 1291 cm^{-1}, observed in the region of the P═O stretch of TMP, can be assigned to the C_3 conformer. The assignment of the lower frequency feature to the lower energy conformer is consistent with the observations of Vidya et al.[10] Using supersonic-jet sampling for matrix isolation, they showed that the higher frequency feature in the region of the P═O stretch was significantly depopulated in the supersonic expansion. This observation clearly established that the lower frequency feature corresponded to the lower energy conformer. The assignment of the 1291 cm^{-1} feature in the vapor phase spectrum to the C_3 conformer implies that our calculated frequency (1401 cm^{-1}) for this conformer is higher than that of the experimental vapor phase value by about 8%. This deviation is in keeping with the general observation that the frequencies calculated at the HF level are generally overestimated by about 10−15%.[17] A scaling factor of 0.92 brings the computed frequency for the C_3 conformer in agreement with the experimental vapor phase value. This scaling factor then brings the computed frequency for the C_1 conformer in excellent agreement with the other experimental feature at 1316 cm^{-1} that can be assigned to the C_1 conformer. The computed frequency of the C_s conformer is close to that of the C_1 conformer. However, since the C_s conformer is only expected to contribute about 5% to the total population, its feature may not be experimentally discernible.

Comparisons of computed frequencies with vapor phase data for the P−O−C modes are not meaningful, since the vapor phase spectrum shown in ref 8 does not afford the resolution to

TABLE 3: Comparison of Experimental and Computed Vibrational Frequencies (cm^{-1}) in TMP

				exptl[a]	
conf	vibrat	HF/6-31G**	MP2/6-31G*	vapor	MI
C_3	P═O	1401 (1287)[b]	1306	1291	1287
	P−(O−C)	1185 (1048)	1090	1060	1048, 1046
	(P−O)−C	936 (866)	872		866
C_1	P═O	1427 (1311)	1332	1316	1302, 1307
	P−(O−C)	1199, 1178 (1060, 1041)	1103, 1086	1060	1061, 1041
	(P−O)−C	932, 917 (861, 848)	868, 850		862, 851
C_s	P═O	1425 (1309)			
	P−(O−C)	1199, 1167 (1060, 1032)			
	(P−O)−C	924, 919 (854, 849)			

[a] Values from refs 8 and 10. [b] Numbers shown in parentheses are scaled frequencies. See text for details on scaling.

discern the features due to the different conformers. Hence these modes must be discussed using matrix isolation data.

Comparison of Matrix Isolation Data with Computed Frequencies. It can be seen that the vibrational frequencies of TMP in the nitrogen matrix shown in Table 2 (taken from refs 8 and 10) are slightly red shifted from vapor phase values. This observation is not surprising since matrix perturbations are known to alter the frequencies in the matrix compared with those of the gas phase values. Hence, to bring the calculated frequencies in agreement with the frequencies obtained in the nitrogen matrix, a different scaling factor from that derived by a comparison with the vapor phase value may have to be used. Furthermore, since matrix perturbations may be different for different modes, it may be necessary to use different scale factors for the different modes.

Figure 2 shows the infrared spectra of TMP trapped in a nitrogen matrix using an effusive (Figure 2, part b) and a supersonic-jet (Figure 2, part c) source. These spectra have been taken from ref 10. The scaled computed frequencies of TMP obtained in this work are also shown in the figure as a stick spectrum (Figure 2, part a).

Even though infrared spectra of TMP were recorded in both argon and nitrogen matrices, we will discuss here the results of TMP trapped in a nitrogen matrix. Infrared spectra of TMP in argon display multiple site effects, complicating assignment, whereas the spectra in a nitrogen matrix are relatively free from multiple site effects.[8]

(a) P═O Vibration: Following an argument similar to that used in assigning the gas phase spectra, the 1287 cm^{-1} feature in the nitrogen matrix can be assigned to the C_3 conformer. This assignment implies that the computed frequency for the C_3 would have to be scaled by a factor of 0.919 to bring the computed frequency in agreement with the experimental feature. (We retain three significant figures for the scaling factor, since it is found to bring the computed features of the C_1 conformer in better agreement with experimental values.) When this factor is used to scale the computed C_1 frequency, the scaled frequency can be seen to agree well with the experimentally observed 1302/1307 doublet. This doublet has been speculated to arise due to multiplet site effect in the nitrogen matrix.[8] Our assignment of the higher frequency feature to the higher energy conformer (C_1) is also consistent with the assignment of Vidya et al.,[10] who showed that the higher frequency feature was significantly depopulated when a supersonic-jet source was used (Figure 2).

(b) P−(O−C) Vibration. Our calculations indicate that this mode appears as a well-split feature in the C_1 conformer but as two nearly degenerate features in the C_3 form. The frequency for the C_3 conformer lies between the two split features of the C_1 conformer. If we therefore assign the 1048 cm^{-1} feature in the nitrogen matrix to the C_3 conformer the computed frequency for this conformer (1185 cm^{-1}) would have to be scaled by 0.884. This scale factor then converts the computed frequencies for the C_1 conformer to 1060 and 1041 cm^{-1}, in excellent agreement with experimental values. Furthermore, Vidya et al. assigned the 1041 cm^{-1} feature to the higher energy conformer, in agreement with our assignment of this feature to the higher energy C_1 conformer.

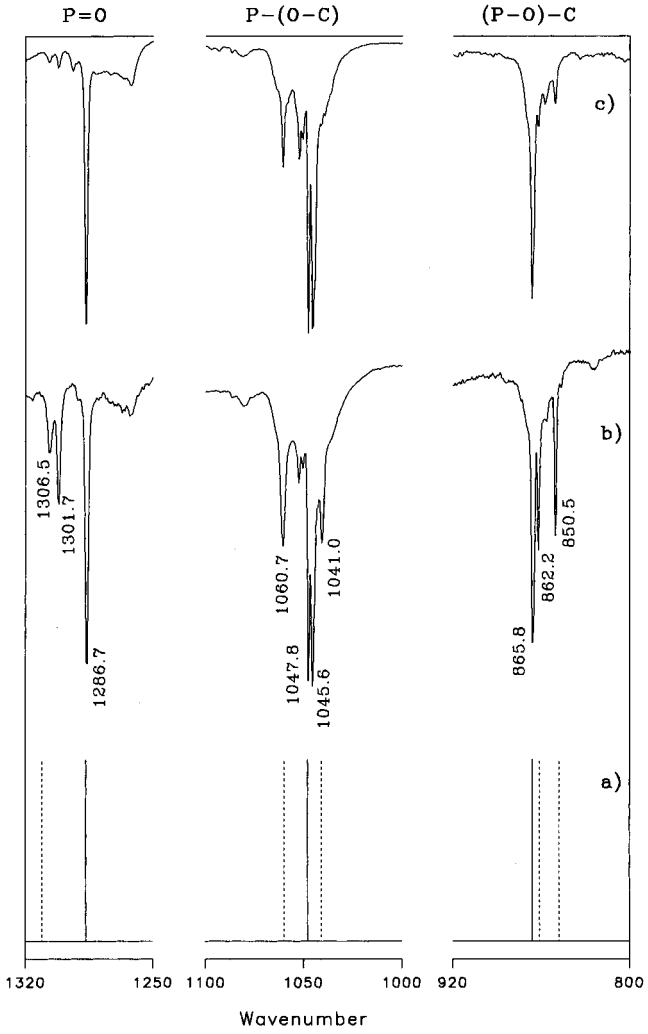

Figure 2. Comparison of (a) scaled HF/6-31G** frequencies with experimental matrix isolation IR data (from ref 10), obtained using (b) an effusive and (c) a supersonic-jet source. Computed IR features of the C_3 conformer are shown in solid lines and those of the C_1 conformer in broken lines.

It must be pointed out that even though the computations indicate that this mode occurs as a nearly doubly degenerate vibration in the C_3 conformer, the experimental feature appears split as 1048/1046 cm^{-1} doublet. This splitting is speculated to be due to site effects.

(c) (P−O)−C Vibration. As with the other P−O−C mode, our calculations indicate that this vibration also occurs as a well-split feature in the C_1 conformer, while it is a nearly doubly degenerate mode in the C_3 conformer. If the experimental feature at 866 cm^{-1} is assigned to the C_3 form, the computed value for this conformer (936 cm^{-1}) would have to be scaled by 0.925. This scaling factor then reduces the computed features for the C_1 conformer to 861 and 848 cm^{-1}, in excellent agreement with the experimentally reported features in the nitrogen matrix. Again, as before, Vidya et al. observed significant depopulation of these features (862 and 851 cm^{-1}) in their supersonic expansion experiments, thus confirming the assignment of these features to the higher energy conformer.

We reiterate that all the features assigned to the C_1 conformer were those that were significantly depopulated in the supersonic expansion−matrix isolation experiments of Vidya et al., as can be seen from Figure 2.

At the MP2/6-31G* level, the calculated frequencies agreed with the experimental values to within ∼4%. Since the discussion of scaling for the MP2 frequencies would be almost identical to the one presented for the HF frequencies, we have not presented the scaling factors separately for the MP2 calculations.

This work coupled with the matrix isolation work of Lisa et al.[8] and Vidya et al.[10] therefore clearly leads to a definitive assignment of the infrared features of the two major conformers in TMP. Our computations and the recently reported supersonic-jet−matrix isolation work[10] indicate that the lowest energy conformer, with the C_3 geometry, has the smallest frequency for the P═O stretch. This observation is also corroborated by the hot nozzle experiments of Sablinskas et al., who showed that on heating the TMP vapors prior to deposition in the matrix, the higher frequency infrared feature increased in intensity. These observations contradict the earlier conclusions of Mortimer[1] that the lower energy conformer had the higher P═O stretching frequency. However, since Mortimer's experiments were done using liquid and solid phase TMP, it would not have been possible for him to discern spectral features due to the individual conformers. Furthermore, problems due to associations might have also complicated his study.

Barrier to Conformer Interconversion. When TMP vapor at room temperature, was trapped in Ar and N_2 matrices at ∼12 K, the conformational population observed in the matrix reflected the temperature of the vapor during deposition. When the matrix was annealed, the different conformers did not interconvert to equilibrate to the low temperature of the matrix.[9,10] Such an observation is taken to indicate that the barrier for conformer interconversion was in excess of 10 kJ/mol (2.4 kcal/mol).[18] However, no direct experimental or computational estimate exists for the barrier to conformer interconversion in TMP. We have therefore computed the barrier at the HF/6-31G** and MP2/6-31G** levels. Since three minima corresponding to C_3, C_1, and C_s symmetries exist in TMP, it would be necessary to probe the conversions $C_1 \leftrightarrow C_3$, $C_s \leftrightarrow C_3$ and $C_s \leftrightarrow C_1$. Since the C_3 and C_1 conformers constitute the major population at ambient temperatures, we have studied the conversion involving the $C_3 \leftrightarrow C_1$ conformers only.

The first step in the barrier calculation was to arrive at the structure of the transition state connecting the two major conformers. The two conformers mainly differed in the value of the O═P−O−C torsional angle. We therefore performed single-point calculations at the HF/6-31G** level, starting from the C_3 conformer and stepping through one of the O═P−O−C torsional angles to eventually arrive at a structure close to the C_1 conformer. The maximum in energy was found to occur near a O═P−O−C torsional angle of 130°. A structure with this torsional angle was then assumed as a starting geometry to *optimize* to a transition state structure, at both HF and MP2 levels. The parameters defining the transition state structure at the MP2/6-31G** level are given in Table 1 and the structure shown in Figure 1. Frequency calculation on the transition state structure was done at the HF/6-31G** level to confirm that the structure corresponded to a first-order saddle point and also to obtain the zero-point energy. (The magnitude of the single imaginary frequency was ∼90 cm^{-1}.) Table 4 gives the energies of the C_3, C_1, and the transition state structures at the HF/6-31G** and MP2/6-31G** levels, together with their zero-point energies calculated at the HF/6-31G** level. The barrier for the $C_1 \rightarrow C_3$ conversion was calculated to be 1.60 kcal/mol at the HF/6-31G** level and 2.20 kcal/mol at the MP2/6-31G** level, after zero-point energy corrections. (When applying the zero-point energy corrections, the computed zero-point values were scaled by 0.92, which brings the calculated HF frequencies in agreement with experimental vapor phase frequencies.) The large barrier for the $C_1 \rightarrow C_3$ conversion is consistent with the observation that the two conformers do not interconvert in the matrix.[9,10] The barrier for the reverse reaction $C_3 \rightarrow C_1$ was 2.62 kcal/mol and 2.76 kcal/mol at the HF and MP2 levels, respectively.

TABLE 4: SCF, MP2, and Unscaled Zero-Point Vibrational Energies (ZPVE) of the C_3, C_1, and Transition State Structure

structure	HF/6-31G** (hartree)	MP2/6-31G** (hartree)	ZPVE (hartree)
C_3	−759.110 80 66	−760.375 604 1	0.144 292 1
C_1	−759.109 240 4	−760.374 761 2	0.144 350 4
transition structure	−759.106 439 6	−760.371 002 8	0.144 076 3

Barrier height for $C_1 \rightarrow C_3$ conversion = 1.60 kcal/mol (HF/6-31G**)
= 2.20 kcal/mol (MP2/6-31G**)

Barrier height for $C_3 \rightarrow C_1$ conversion = 2.62 kcal/mol (HF/6-31G**)
= 2.76 kcal/mol (MP2/6-31G**)

Conclusions

Clearly, this work, together with the matrix isolation work reported earlier,[8,10] has led to a clearer understanding of the spectra, structure, and other molecular properties of TMP.

In TMP, three minima, in order of increasing energy, corresponding to C_3, C_1, and C_s symmetries, were found, using the 6-31G* and 6-31G** basis sets, both at the HF and MP2 levels. The energy ordering of the conformers obtained in this study is different from that obtained in earlier ab initio studies. We also report the occurrence of a minimum corresponding to a C_s symmetry not reported earlier. As is generally observed, the lower energy conformer also had a smaller dipole moment when compared with the other conformers.

Vibrational frequencies of the P═O and P−O−C modes, calculated at the HF and MP2 level, agreed well with experimental frequencies. This work has led to a definitive assignment of the various infrared features observed in the matrix isolation spectra. The lowest energy conformer with a C_3 symmetry had the lowest P═O frequency compared with that for the higher energy C_1 and C_s conformers, a conclusion that differs from an earlier report.

The energy barrier for conformer interconversion between the two conformers C_1 and C_3 was calculated to be 2.20 and 2.76 kcal/mol for the $C_1 \rightarrow C_3$ and $C_3 \rightarrow C_1$ conversions, respectively. This value is consistent with the observation that the conformers do not interconvert in the matrix on annealing.

Acknowledgment. L.G. gratefully acknowledges the Research Fellowship awarded by the Council of Scientific and Industrial Research, India. A gift of a workstation from Alexander von Humboldt Foundation (Germany) at IIT, Madras, is acknowledged with thanks.

References and Notes

(1) Mortimer, F. S. *Spectrochim. Acta* **1957**, *9*, 270.
(2) Maiants, L. S.; Popov, E. M.; Kabachnik, M. I. *Opt. Spectrosc.* **1959**, *7*, 108.
(3) Popov, E. M.; Kabachnik, M. I.; Mayants, L. S. *Russ. Chem. Rev.* **1961**, *30*, 362.
(4) Herail, F. M. *J. Chim. Phys. Phys.-Chim. Biol.* **1971**, *68*, 274.
(5) Khetrapal, C. L.; Govil, G.; Yeh, H. J. C. *J. Mol. Struct.* **1984**, *116*, 303.
(6) Van Wazer, J. R.; Ewig, C. S. *J. Am. Chem. Soc.* **1986**, *108*, 4354.
(7) Taga, K.; Hirabayashi, N.; Yoshida, T.; Okabayashi, H. *J. Mol. Struct.* **1989**, *212*, 157.
(8) Lisa, G.; Sankaran, K.; Viswanathan, K. S.; Mathews, C. K. *Appl. Spectrosc.* **1994**, *47*, 8.
(9) Sablinskas, V.; Horn, A.; Klaeboe, P. *J. Mol. Struct.* **1995**, *349*, 157.
(10) Vidya, V.; Sankaran, K.; Viswanathan, K. S. *Chem. Phys. Lett.* **1996**, *258*, 113.
(11) Frisch, M. J.; Trucks, G. W.; Head-Gordon, M.; Gill, P. M. W.; Wong, M. W.; Foresman, J. B.; Johnson, B. G.; Schlegel, H. B.; Robb, M. A.; Replogle, E. S.; Gomperts, R.; Andres, J. L.; Raghavachari, K.; Binkley, J. S.; Gonzalez, C.; Martin, R. L.; Fox, D. J.; Defrees, D. J.; Baker, J.; Stewart, J. J. P.; Pople, J. A., Gaussian, Inc., Pittsburgh, PA, 1992.
(12) Raevsky, O. A. *J. Mol. Struct.* **1973**, *19*, 275.
(13) Minkin, V. I.; Osipov, O. A.; Zhdanov, Yu. A. *Dipole Moments in Organic Chemistry*; Plenum Press: New York, 1970.
(14) Lisa G.; Sankaran, K.; Viswanathan, K. S.; Mathews, C. K. *Appl. Spectrosc.* **1994**, *48*, 801.
(15) Lisa G.; Sankaran, K.; Viswanathan, K. S.; Mathews, C. K. *Spectrochim. Acta* **1995**, *51A*, 587.
(16) Lisa G. Ph. D. Thesis, University of Madras, 1993.
(17) Hehre, W. J.; Radom, L.; Schleyer, P. R.; Pople, J. A. *Ab initio Molecular Orbital Theory*; John Wiley & Sons: New York, 1986.
(18) Barnes, A. J. In *Matrix Isolation Spectroscopy*; Barnes, A. J., Orville-Thomas, W. J., Muller, A., Gaufres, R., Eds.; D. Reidel Publishing Co.: Holland, 1981; Chapter 23.